

THE COMPLEX SUN: TURBULENCE AND COMPLEXITY IN THE SOLAR ATMOSPHERE

R. T. James McAteer^{1,2}, Peter T. Gallagher³, Ireland, J.^{4,2}, Young, C. Alex^{4,2}, Hewett, Russell J.⁵, and Conlon, P.⁶

¹*Catholic University of America, Work carried out as NRC and ORAU Research Associate*

²*NASA/Goddard Space Flight Centre, Greenbelt, MD, 20771*

³*Trinity College Dublin, Dublin 2, Ireland*

⁴*L-3 Communications, GSI*

⁵*University of Illinois at Urbana-Champaign, MC 258, Urbana, IL 61801*

⁶*Paul's address*

ABSTRACT

It is already understood that simple monofractal and Fourier studies of magnetic field data give a good, though imperfect, understanding of active region complexity. We extend this work by reviewing multiscale and multifractal approaches to quantify magnetic complexity; presented and discussed in relation to understanding and characterizing solar active region magnetic field configurations and predicting solar activity. These differing, but complimentary approaches, will be a vital component in understanding active region evolution and providing space weather predictions.

Key words: Solar magnetic fields; Image processing; Space Weather.

1. INTRODUCTION

Solar flares are among the most energetic events in the solar system and have intrigued generations of physicists. These events influence a panorama of physical systems, from the photosphere of the Sun, through the heliosphere and into geospace. Although flares occur in active regions in the solar corona, active regions are stressed through evolution of the magnetic field configuration in the photosphere. Active regions are formed through the convective action of subsurface fluid motions pushing magnetic flux tubes through the photosphere. The active region flux tubes are jostled around by turbulent photospheric and sub-photospheric motions, and when conditions are right, the active region produces a flare. The precise conditions required to create these enormously energetic events are as yet unknown. Understanding this interaction is of considerable practical importance because technological systems, such as communications and navigation satellites, can suffer interruptions or permanent damage. Adverse effects from space weather include failure and loss of satellites, airline communication interruptions, GPS sig-

nal degradation, and electric utility faults.

Through characterizing active region magnetic field complexity we can begin to understand which active region properties are important indicators of their activity. The algorithms described below represent novel approaches to analysing longitudinal magnetogram data and aim to generate physically motivated complexity measures. Since Kolmogorov (1941) and Mandelbrot (1977) first introduced the ideas of turbulence and fractals, respectively, complex systems have been found to ubiquitous in many areas of human and natural sciences. It is envisaged that the holistic opportunities of the multifractal and multiscale algorithms proposed here will be useful in all studies of complex systems, turbulence and fluid dynamics (e.g., heartbeat dynamics, hydrology)

2. METHODS

The power-law frequency distribution of flares (Dennis, 1985) and active regions (Harvey & Zwaan, 1993) is a clear signature of the self-organised criticality of active regions as externally driven, dissipative, dynamical systems. The system arises from competition between the input (flux emergence and rearrangement in the photosphere) and output (electrical current build up and resistive dissipation) in the corona. Although localised, this redistribution affects neighbouring regions and an avalanche occurs (Vlahos & Georgoulis, 1995). As flares are powered from the stressed field rooted in the photosphere, a study of the photospheric magnetic field complexity may provide a clearer understanding of the non-linear physics at play, and hence a quantitative flare prediction system.

A few studies have been made of coronal activity and their concomitant photospheric field distributions. While traditional Fourier and fractal methods have been used extensively in image processing, and are well understood, they do not provide a complete diagnostic of the range of spatial frequencies or scales within an image. As such,

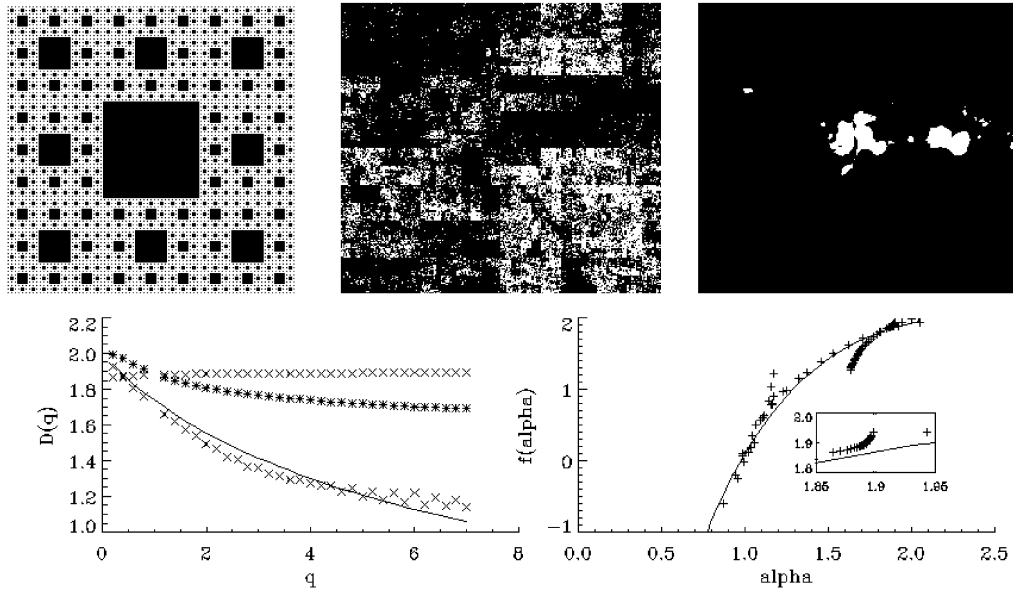


Figure 1. Top: (left) A computer generated monofractal, (middle) a computer generated multifractal, right (active region magnetogram). Bottom: The D_q (left) and $f(\alpha)$ (right) spectra of the monofractal (blue), the multifractal (red crosses - calculated values, red line - actual spectra) and magnetogram (black). The magnetogram displays the multifractal signature of a steadily decreasing D_q and wide, non-localized, $f(\alpha)$, as expected from a fully developed turbulent system.

a consistent, causal relationship between photospheric field conditions and activity is unknown. It is clear that there is an outstanding need for a comprehensive and wide ranging approach to the understanding of complex magnetic fields and their association with activity. This paper discusses two complimentary techniques, namely multiscalar and multifractal methods. Both methods are based on the premise that physical systems cannot be adequately described by simple parameters, but require methods that capture their true complexity as a function of size scale.

2.1. Multifractals

The fractal dimension of any object can be thought of as the self-similarity of an image across all scale sizes, or the scaling index of any length to area measure,

$$A \propto l^\alpha, \quad (1)$$

where α is the Hölder exponent. McAteer et al. (2005) showed that the study of active region magnetic field fractal dimension produces a significant, although incomplete, predictor of solar flares. Previous work (Lawrence et al., 1995; Georgoulis, 2005; Abramenko, 2005) discusses the complexity of magnetic field data via a multifractal analysis. A multifractal system will contain a spectrum of fractal indices of different powers,

$$A \propto l^{f(\alpha)}, \quad (2)$$

and takes account of the measure at each point in space. Any measure distribution (e.g. magnetic field in an im-

age) can be characterized by

$$\phi(q, \tau) = E \sum_{i=1}^N P_i^q \varepsilon^{-\tau}, \quad (3)$$

where q, τ can be any real numbers, and E is the expectation of the object consisting of N parts. In this form, ϕ is the coupled τ -moment of the size ε , and q -moment of the measure P . The three main multifractal indices commonly used to represent a non-uniform measure are then:

- Generalised Correlation dimensions, $D_q = \frac{\tau}{(q-1)}$;
- Hölder exponent, $\alpha = \frac{d\tau}{dq}$;
- Legendre transformed $f(\alpha) = q\alpha - \tau$

When applied to a traditional box-counting approach, it is useful to define the partition function, $Z_q(\varepsilon) = \sum_{i=1}^N P_i^q(\varepsilon)$, such that $\tau(q) = \lim_{\varepsilon \rightarrow 0} \log Z / \log \varepsilon$, and any of the three representations above can be calculated. The terminology used in this description is deliberately similar to that used in turbulence studies. Figure 1 (left) shows a comparison of the D_q and $f(\alpha)$ indices for a monofractal (left; the Sierpinski carpet), a multifractal (middle), and a solar active region magnetogram (right). The monofractal (blue X) exhibits a flat D_q (~ 1.89) spectrum and narrow $f(\alpha)$ spectrum whilst the multifractal (red X) exhibits a monotonically decreasing D_q spectrum (for increasing q) and wide $f(\alpha)$ spectrum.

The magnetogram (black *) exhibits a similar multifractal behaviour. The degree of multifractality of an image

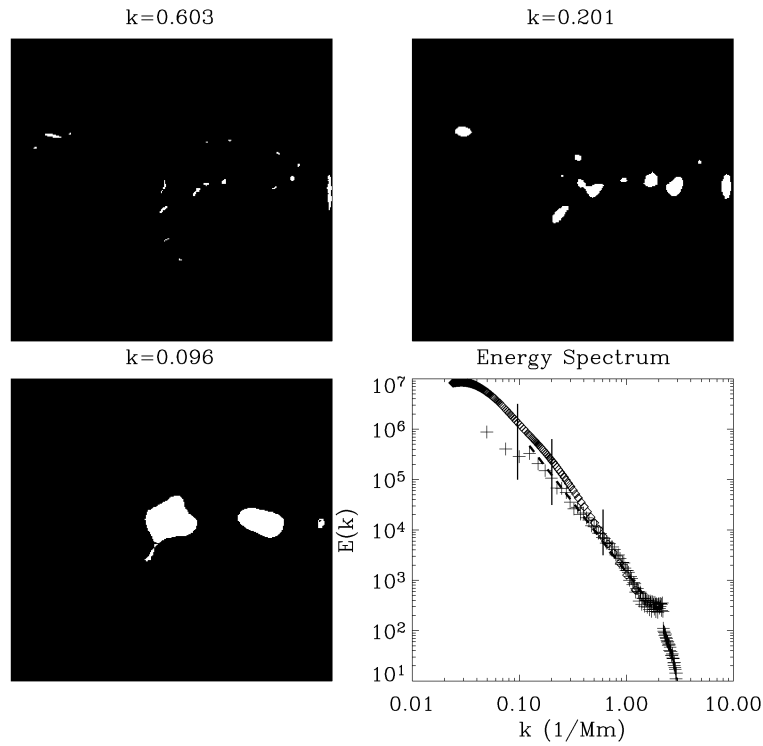


Figure 2. The wavelet decomposition of the magnetogram in Figure 1, at three different scales. The wavelet energy spectrum (lower right, black diamonds) agrees well with the Fourier spectrum (blue crosses). The green vertical lines are at the wavenumber of each scale displayed.

can be measured as the drop of the D_q or width of the $f(\alpha)$ spectrum. Multifractal measures can be directly compared to self-similar cascade or self-organised criticality models, both of which have been used to model energy release in solar flares.

2.2. Multiscale Measures

A competition between energy input (large scales) and turbulent diffusion (small scales) leads to a stationary turbulent regime with constant energy transfer rate. The energy, E , at scales (frequency k) produced in fully developed turbulence was predicted by Kolmogorov (1941) to scale as

$$E(k) \propto k^{-5/3}, \quad (4)$$

Nakagawa & Priest (1973) showed that the magnetic power spectra of an active region scaled as ~ -1 . Abramenko (2001) found a spectral index closer to the Kolmogorov value of $-5/3$. A comparison of 16 active region from hi-res MDI data showed a correlation between larger absolute spectral index and flaring activity; regions with Fourier spectral indices much less than $-5/3$ tended to produce more larger flares (Abramenko, 2005b). However, Fourier analysis loses any spatial information of the image, essentially providing a global indication of complexity. In solar physics, the local information is essential as small regions of flux emergence/submergence are vital

in detailing the evolution of the surface sources of space weather applications. Wavelet analysis, however, retains the localized spatial information, providing vital information on the turbulent flow. The continuous wavelet transform of an image, $I(r)$, can be defined as

$$w(s, x) = \frac{1}{s^{0.5}} \int_{-\infty}^{\infty} I(r) \psi^* \frac{r-x}{s} d^2 r, \quad (5)$$

where $\psi(r)$ is the mother wavelet, scaled (s) and dilated (x), and w are the wavelet coefficients. Figure 2 shows the wavelet decomposition at three spatial scales of the same active region as Figure 1 (right), along with a comparison of the global wavelet analysis and traditional Fourier approach. Wavelet analysis retains the localized spatial information, providing vital information on the turbulent flow. The mother wavelet can take several forms, depending on the application. A derivative of Gaussian wavelet is useful for detecting sudden local changes in an image, hence this can be used to detect the neutral line position and magnitude. A Haar wavelet is useful in detecting and removing the intermittent component an image, a vital tool in describing bursty behaviour. A discrete (e.g., à trous) wavelet can be used to efficiently detect flux emergence as a function of size scale. Other multiscale methods (e.g., shapelets, curvelets) may also provide efficient analysis tools.

3. CONCLUSIONS

Image processing techniques already prevalent in other fields can be readily applied to, and hence will become a vital component of, solar physics data analysis. In this review we have examined two instances of how advanced techniques can produce physically motivated parameters, complimenting existing analysis techniques. Although applied to magnetic field data, these techniques are already gaining prevalence in all areas of solar physics, from multiscale CME detection (Stenborg & Cobelli, 2003; Young & Gallagher, 2006) to quantify the memory of HXR flare lightcurves (McAteer et al., 2006) and employing wavelet phase analysis in studying quiet Sun oscillations (Bloomfield et al., 2004). In the future we wish to employ a two strand approach: apply these techniques to the large available SoHO MDI dataset to search for a correlation with solar flares; apply these techniques to models of active region magnetic field evolution to give a deeper causal understanding of the non-linear physics involved. Combined with the wealth of new data from Solar-B and STEREO, a reliable and timely space weather prediction system may soon be available.

ACKNOWLEDGMENTS

JMA is grateful for a Research Associateship from the National Research Council and resources from the RHESSI group at GSFC to carry out this work. This work was also supported by a NASA LWS grant and Dr Gurman at GSFC in support of *Solarmonitor.org*.

REFERENCES

- Abramenko, V. I., Yurchyshyn, V. B., Wang, H., & Goode, P. R. 2001, *Sol. Phys.*, 201, 225
- Abramenko, V.I. 2005, *Sol. Phys.*, 228, 29
- Abramenko, V.I. 2005b, *ApJ*, 629, 1141
- Bloomfield, D. S., McAteer, R. T. J., Lites, B.W., Judge, P.G., Mathioudakis, M., & Keenan, F.P., 2004, *ApJ*, 617, 623
- Dennis, B.R. 1985, *Sol. Phys.*, 100, 465
- Georgoulis, M. 2005, *Sol. Phys.*, 228, 5
- Harvey, K.L., & Zwaan, C. 1993, *Sol. Phys.*, 148, 85
- Kolmogorov, A.N. 1941, *C. R. Acad. Sci. USSR*, 30, 301
- Lawrence, C.A. & Ruzmaikin 1995, *Phys. Rev. E*, 51, 316
- Mandelbrot 1977, *Fractals* (San Francisco: Freeman)
- McAteer, R.T.J., Gallagher, P.T., & 2005, 631, 628
- McAteer, R.T.J., Young, C.A., Ireland, J., & Gallagher, P.T. 2006, in prep
- Nakagawa, Y., & Priest, E. R. 1973, *ApJ*, 179, 949
- Stenborg, G., & Cobelli, P.J. 2003, *A&A*, 398, 1185

Vhalos, L., Georgoulis, M., Kluving, R., & Paschos, P. 1995, *A&A*, 299, 897

Young, C.A. & Gallagher, P.T. 2006, in prep